MECSOL 2022 - Proceedings of the 8th International Symposium on Solid Mechanics
M.L. Bittencourt, J. Labaki, L.C.M. Vieira Jr. and E. Mesquita (Editors), Campinas SP, Brazil, October 17th to 19th, 2022

PLASTICITY EFFECT ON FATIGUE LIFE OF AERONAUTICAL STRUCTURES CONSIDERING A VARIABLE AMPLITUDE LOADING

Natan Santos dos Reis [1], Mariano Andrés Arbelo [1], Carlos Eduardo Chaves [2]

[1] ITA – Instituto Tecnológico de Aeronáutica, Praça Marechal Eduardo Gomes, 50 - Vila das Acacias, São José dos Campos

[2] Embraer, Av. Brg. Faria Lima, 2170 - Putim, São José dos Campos

Abstract: This work analyzes the effect of plasticity in the fatigue life of aeronautical structures that experience a variable loading scenario, by comparing a strain-based fatigue approach against a classical stress-based fatigue approach, which is lately modified to account for plastic deformation through a simple plasticity correction model. This work uses a representative loading scenario based on what airplanes experience throughout their operational life, by implementing the standardize TWIST loading sequence. Moreover, the MINITWIST was used to verify the impact of a reduced spectrum that intends to be more suitable for testing. The material analyzed was aluminum 2024-T351 alloy and the geometry considered was an open-hole plate with 5 different stress concentration factors (1.0, 2.0, 2.5, 3.0, 3.33) in order to obtain a wide range of results. Rainflow cycle counting method is used to quantify the number of cycles per flight. A stress-life curve coupled to the Smith-Watson-Topper's mean stress correction and the Palmgren-Miner cumulative damage rule is used to determine the total fatigue damage. In addition, plastic deformation effects are accounted by adjusting the maximum stresses of cycles who overcome the material yield strength, using Neuber's rule and Ramberg-Osgood equations iteratively. The numerical results show that, for the proposed loading spectra, the consideration of plasticity effects have increased the fatigue life by approximately 23% for the maximum stress concentration factor of 3.33 but have no impact for the minimum stress concentration factor of 1.0 where plastic deformations didn't happen. Besides that, the use of MINITWIST loading spectra presented similar results of fatigue life compared to the TWIST loading sequence, indicating that small amplitude load cycles do not affect much in fatigue life.

Keywords: TWIST fatigue method, strain-based fatigue approach, variable amplitude loading.)

INTRODUCTION

To certify an aircraft, it is necessary to follow the regulations of the regions this product is going to operate. The world's largest civil aviation market is the United States according to Embraer (Market Outlook 2019-2038). FAA (Federal Aviation Administration) is the American organization responsible to regulate all aspects of civil aviation. One of the demands for commercial airplanes is to ensure that the aircraft will not suffer catastrophic damage due to fatigue during its operational life.

The fatigue life of a structure depends on aspects such as material, geometry, loads and external agents (temperature, corrosion, among others). Most airplane structures experience a variable loading scenario, and the fatigue damage estimation for each cycle can be done in different ways. As presented in Moreira (2020), plastic deformations may have a considerable impact in fatigue life of aluminum structures. These deformations may occur in localized regions where fatigue cracks begin, and in the presence of compressive residual stresses it slows crack growth and increase fatigue life. To better understand the impact of considering plastic deformations in fatigue life, this work intends to estimate the fatigue life of a structure using the Palmgren-Miner cumulative damage rule, with and without a plasticity correction method in cycles which yield stress is exceeded and compare it to an approach that considers the plastic deformation and its effects in fatigue life. To reach these objectives a representative fatigue spectrum for a particular aircraft is used to estimate fatigue life using both methods.

There are different approaches and theories that can be used to estimate fatigue failure, some theories were developed for a multiaxial analysis as Branco (Branco, et al., 2021) presented a comparison of different one-parameter damage laws and local stress-strain approaches of notched components. Liao (Liao, et al., 2020) also published a review on notch effects on metal fatigue but discuss uniaxial and multiaxial loading scenarios. By dividing the theories in four categories, namely, nominal stress approaches (NSA), local stress-strain approaches (LSSA), critical distance theories

and weighting control parameters-based approaches. Liao, et al., introduced methods to estimate fatigue failure considering notch effects.

In this work NSA and LSSA approaches were used and some theories on those methods will be discussed. Starting with NSA methods, they utilize S-N curves to obtain the life for each cycle and these curves can be based directly on notched specimens or adjusted through stress concentration factors. Some researches on these subject are the two-parameter nominal stress approach developed by Qiao (Qiao, et al., 1995), the new prediction approach based on multi-factor correction by Guanglin (Guanglin, et al., 2018) and the study of the effect of holes quality on fatigue life of open hole made by Liu (Liu, et al., 2007).

When considering a LSSA approaches, the estimation of fatigue failure considers that fatigue strength and lifetime of notched components are governed by the maximum local stresses and strains at the notch tip (Liao, et al., 2020). For these approaches it's common to occur plastic deformations on the structure, thus is important to have equations that can correctly identify the material's mechanical behavior before and after the yield strength. The first step is to establish the stress-strain relation, and it can be done by using approximation calculations, generating experimental data or using elastic-plastic FEA approaches. Some examples are the fatigue life evaluation made by Chen (Chen j, et al., 2020) in which Neuber's model was used to calculate local stress and strain, the development of a framework made by Zhao (Y.X. Zhao, et al., 2008) that performs a strain-based fatigue reliability analysis by generating test data to correlate the stress and strain, and the study of Belkhiria (Belkhiria, et al., 2020) where the correlation is made through ABAQUS software.

After the calculation of stress and strain a cycle counting method is applied to analyze every cycle of the loading sequence. With this second step concluded, the mean stress effect must be considered to get the number of cycles to failure and the damage be identified. For the mean stress correction be implemented in a strain-life curve, Dowling (Dowling, 2009) discussed the applicability of a few equations and indicated there benefits. To compute the damage of a cycle there are many damage rule theories, even though the Palmgren-Miner rule is widely implemented. Some examples were described by Zhou (Jie Zhou, et al., 2020) when he presented a novel non-linear cumulative fatigue damage rule, such as Kwofie's model (Kwofie, 2013) and Rege's model (Rege and Pavlou, 2017). Approaches developed by Peng (Peng, et al., 2018) and Böhm (Böhm, Kurek, et al., 2014) introduced terms to account the material memory effect.

In aircraft industry, to have a good prediction of fatigue life not only the value of stresses must be well considered but likewise the load spectra. The differences in the upper part of the gust load frequency distribution diagrams used in tests are apparently one of the reasons for the large discrepancies between results obtained in different laboratories (Buch, 1980). Thus, a wide range of standardized load sequences have been developed for different purposes. In Heuler; Klätschke (Heuler and Klätschke, 2005) a compilation and discussion of these methods was conducted giving an overview on this topic. Moreover, studies involving the generation of standardized load sequences still being developed for different purposes such as Shanshan's procedure (Li, 2016).

In many transport aircrafts a critical area regarding fatigue turns out to be the lower wing skin at the wing root. Consequently, TWIST was developed as a standardized load sequence that would be representative for the load-time history in the wing root of transport aircraft (De jong, 1973). TWIST method was published in 1973 and thenceforth it widespread and several requests for a shortened version were expressed. Therefore, National Aerospace Laboratory (NLR; Dutch: Nationaal Lucht- en Ruimtevaartlaboratorium) and Laboratorium für Betriebsfestigkeit (LBF) established a shortened version called MINITWIST, to reduce testing time and costs (Lowak, 1979).

For highly irregular variations of load with time, it is not obvious how individual events should be isolated and defined as cycles so that the Palmgren–Miner cumulative damage rule can be employed. However, a consensus has emerged that the best approach is a procedure called rainflow cycle counting. (Dowling, 2012)

A few different terms have been employed in the literature to designate cycle-counting methods which are similar to the rainflow method. If the load history begins and ends with its maximum peak, or with its minimum valley, all of these give identical counts. In other cases, the counts are similar, but not generally identical (ASTM, 2011). Due to the similarity in counts results and the rainflow being largely implemented, the rainflow cycle-counting method is the most appropriate choice.

For a notched structure under cyclic loading with high loads yielding can happen, in case a reversion in direction of straining occurs after the yielding the stress-strain path will be different from the initial monotonic. The yield strength in this reversed direction is lower and this is called Bauschinger effect. Schijve (Schijve, 2009) says that local plastic deformation may cause an irregular residual stress distribution. In some cases, these residual stresses can present compressive behavior, leading to a change in fatigue damage caused by subsequent cycles when compared to what they would cause if there were no residual stresses. To estimate this, several damage fatigue calculation methods have evolved and been developed for a large array of materials. A well-known model is the Palmgren-Miner rule which was first expressed by Miner in 1945 (Fatemi, 1998), which 5 years ago was still being recommended as the model to calculate fatigue damage of steel structures by design standards such as DNVGL-RP-C203 (Rege, 2017). Since the Palmgren-Miner rule has shown conservative results when increasing loading amplitude, more recent approaches for

cumulative damage have been presented looking to solve this problem. To name a few, there's Peng's rule (Peng, 2018) and Rege's model (Rege, 2017).

Not only the workflow of analysis must be discussed but also the material's mechanical behavior. The stress – strain relation in metallic materials is approximately linear up to the yield strength, in a region where only elastic deformations occur. Beyond this limit, the correlation is no longer linear. To represent this effect Ramberg-Osgood equation is largely used. Since the conditions this structure operates in a variable loading scenario, local plasticity may occur around notches due to elevated stress concentration factors, therefore, it is important to evaluate in detail this behavior. To determine notch strain during plastic deformations few closed solutions exist. One way to analyze these local strains is to use Neuber's rule (Neuber, 1961), an approximate method to estimate stress and strains at notches.

Considering the scenarios presented above, this work main objective is to understand the effect of plasticity in aeronautical structures with variable amplitude loading by comparing three different fatigue life estimation methods. To reach this objective, the tasks sequence was estimate the fatigue life using a representative commercial airplane loading sequence (the TWIST and MINITWIST), estimate the fatigue life with two stress-based approaches and one strain-based approach by developing methodologies based on stresses and strains, adding a hybrid approach that uses the stress criterion coupled with the correction of cycles that present plastic strain, and analyze the results of the three different fatigue life estimation methods. This is done considering Al2024-T351 as the material analyzed and stress concentration factors of 1.0, 2.0, 2.5, 3.0 and 3.33.

.

Methodology

In this work three different methodologies will be implemented, tested and compared using a common use case. The first one is strain-based and the other two using the S-N curve coupled with SWT's equation for mean stress correction. The difference between the two stress-based approaches is that one takes into account the plastic effects by simple corrections and the other does not. All methods use the Palmgreen-Miner cumulative damage rule for fatigue life estimation, since this rule is largely tested providing more studies and results, and the standardized load sequence is based on TWIST methodology for all cases.

Material properties

The material selected was the Al 2024-T351 and the properties were based on Dowling (Dowling, 2012). Aluminum alloys, such as 2XXX series (Al-Cu-Mg), are the most used material in aeronautical industry due to their strength-to-weight relation. Of these, the most used is the Al2024 (Maduro, 2011). Garcia (M. García-Rubio, 2009) quotes a similar commentary made by J. Jones (1990) saying that "Aluminium 2xxx series alloys are widely used in the aerospace industry due to their low density and high specific strength".

Another reason the Al2024 is extensively used in aeronautical industry, as discussed by Schijve (Schijve, 1994) when analyzing some aircraft fatigue accidents, is due to being less crack-sensitive than other aluminum alloys, such as 7075-T6. Consequently, Al2024 sheet material is often used in riveted lap joints.

With the purpose of estimating the fatigue life, the material strain-life curve is needed. Therefore, the tensile properties and strain-life constants of the 2024-T351 are presented in Tab. 1 and were taken from Dowling (Dowling, 2012).

Table 1 – Material properties (Dowling, 2012).

Material	σ_0 (MPa)	E (GPa)	H' (MPa)	n'	σ'_f (MPa)	B	ε'_f	c
Al2024-T351	379	73.1	662	0.070	927	-0.113	0.409	-0.713

Where σ_0 is the yield strength, E is the elasticity modulus, H' is the strength coefficient for stress-strain curves, n' is the strain hardening exponent of Ramberg-Osgood equation, ε'_f, σ'_f, B and c are constants fitted from the material ε-N curve.

Different stress concentration factors (k_t) were used aiming a wider range of cases to have more data to be analyzed. The mean stress definition will be explained in section 2.2, but assuming the structure shouldn't experience plastic deformations during less severe flight types (type H, I and J), the higher k_t adopted was 3.33. Thus, the k_t values used for this study are presented in Tab. 2.

Table 2 – Stress concentration factors analyzed.

Study case	1° case	2° case	3° case	4° case	5° case
Stress concentration	1.0	2.0	2.5	3.0	3.33

Spectrum generation

The procedure of generating the spectrum was divided for each flight stage, taxi, takeoff/landing roll and airborne. The report made by Skinn (Skinn, 1996) was used to acquire the load factor spectra data. Before initiating the analysis, an important parameter needs to be determined. Since the structural element was not defined, the one-g stress tension (S_{1g}) was select as 85 MPa. This previous definition means that during a straight-and-level flight the structure will be experiencing this tension stress, and any additional stress caused by an incremental load factor is going to be proportional to 85 MPa. Following TWIST methodology when analyzing the airplane wing root stresses, the ground mean stress is selected as -0,3 of flight mean stress (S_m). Moreover, the stress concentration factor must also be considered, thus the one-g tension stress increases in accordance with the concentration factor.

The types of airborne loads considered in this work are related to departure, climb, cruise, descent and approach. The absolute values are presented in Tab. 3.

Table 3 – Block flight data

N° of flights in a block	4000	Dimensionless
airborne time per flight	1.53	hours
total airborne time	6113.64	hours
roll time per flight	0.017	hours
total roll time	68	hours
taxi time per flight	0.25	hours

After getting the incremental load factor data for every stage, the stress can be calculated as shown in the equation below

$$S = S_{1g}(1 + \Delta n_z) \tag{1}$$

where S_{1g} is the nominal stress in one g operation and Δn_z is the incremental load factor in the vertical direction of the airplane. With the stress values and their respective exceedance, the stresses are separated in two branches as Fig. 1 shows for airborne, one contains the higher stress levels while the other possess the lower stress levels.

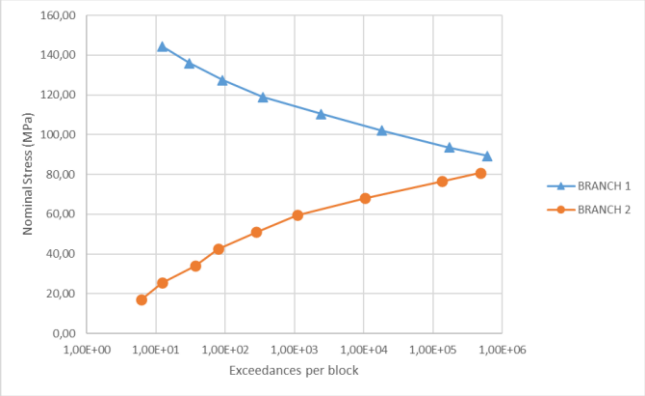

Figure 1 – Airborne spectrum converted to nominal stress

The steps taken to generate the roll and taxi spectrum were the same as presented for the airborne, the only difference is that they are based on different stages data.

Spectrum discretization

After generating the loading spectra presented in previous section, the cumulative number of times a load level is reached, called exceedance, were defined in accordance with TWIST method as shown in Fig. 2. This approach creates discretized load levels to simulate the real loading scenario. Since the original method described the exceedances only for gust loads, this study adopted this distribution for airborne, taxi and roll loads.

Flight type	Number of flights in one block of 4000 flights	Number of gust loads (full cycles) at the 10 amplitude levels										Totale number of cycles per flight
		I	II	III	IV	V	VI	VII	VIII	IX	X	
A	1	1	1	1	4	8	18	64	112	391	900	1500
B	1		1	1	2	5	11	39	76	366	899	1400
C	3			1	1	2	7	22	61	277	879	1250
D	9				1	1	2	14	44	108	680	950
E	24					1	1	6	24	165	603	800
F	60						1	3	19	115	512	650
G	181							1	7	70	412	490
H	420								1	16	233	250
I	1090									1	69	70
J	2211										25	25
Total number of cycles per block of 4000 flights		1	2	5	18	52	152	800	4170	34800	358665	
Cumulative number of load cycles per block of 4000 fl.		1	3	8	26	78	230	1030	5200	40000	398665	

Figure 2 – TWIST definition of flight types and number of load cycles within each flight (De Jong, 1973)

Interpolations have been conducted encountering the stress in which their exceedance is the same as the one defined in TWIST for each load level and flight type.

The interpolated stress is given by

$$\sigma = \sigma_{sup} + \left(\frac{\sigma_{inf}-\sigma_{sup}}{\log(exc_{inf})-\log(exc_{sup})}\right) * \left(\log(exc) - \log(exc_{sup})\right) \quad (2)$$

where σ_{sup} is the first superior stress threshold, σ_{inf} is the first inferior stress threshold, exc_{sup} is the first superior exceedance threshold, exc_{inf} is the first inferior exceedance threshold and exc is the exceedance defined for the load cycle level. Using the stresses found with this interpolation, Fig. 3 shows the discretization obtained for airborne.

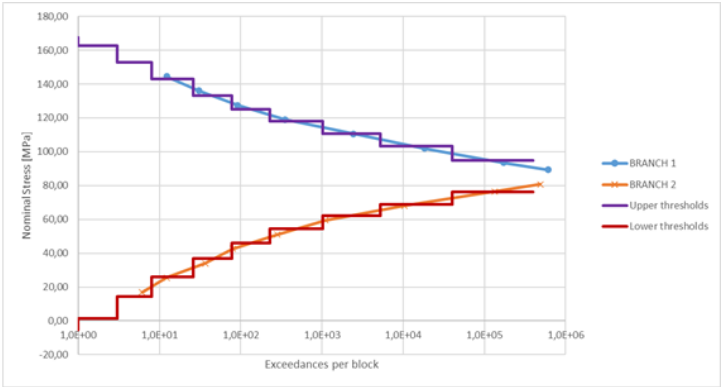

Figure 3 – Airborne spectrum discretization

As explain previously, MINITWIST is a shortened version of TWIST that also intends to generate a representative fatigue spectrum for transport aircraft. Knowing it can reach a similar result with a shorter testing time in some cases, it was decided to also use this method. So, the values of the discretized spectra generated in this section are used for MINITWIST as well.

This procedure was also made to discretize the stresses for taxi and roll operations. By pairing the stress from the two curves that have the same exceedance.is possible to define cycles for each flight stage.

After discretizing the load cycles of each stage, these load groups were aligned following the flight stages presented in Fig. 4, to generate the flight load sequences and then go through a rainflow cycle counting method, having as output

the count, the stress range, and the mean stress of each cycle of all ten flight types. In real life the sequence of loads is random, but to evaluate the maximum impact that plasticity could have within a flight, the code distribution started each stage with the highest load level and decreases until reaches the lower level that appears in the stage.

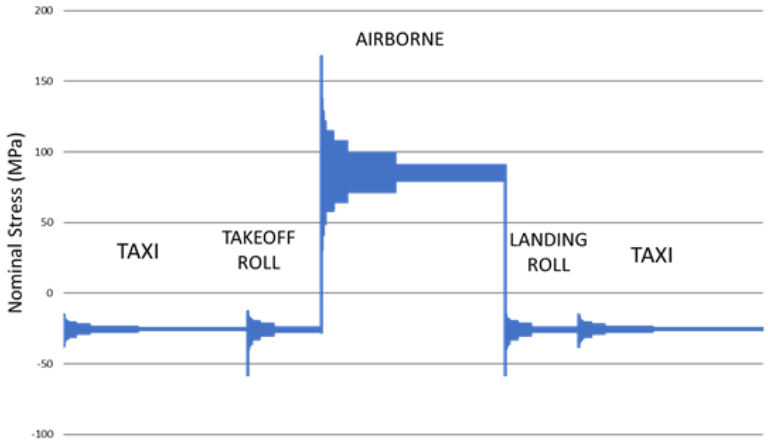

Figure 4 – Load sequence for TWIST flight type A.

Fatigue life estimation using S-N curve without plasticity correction

The first method selected to estimate the fatigue life of this variable amplitude loading scenario is the S-N curve with SWT's equation for mean stress correction and the Palmgren-Miner cumulative damage rule. Using the output data from the rainflow and the material properties discussed in the previous section, the fatigue life was estimated. The reversible amplitude nominal stress was calculated using the maximum nominal stress and the stress amplitude as shown in equation below.

$$S_{ar} = \sqrt{S_{max} S_a} \tag{3}$$

Then, the number of cycles to failure for a particular cycle is determined.

$$N_f = \left(\frac{S_{ar}}{A/k_t}\right)^{1/B} \tag{4}$$

where $A = (2^B)\sigma'_f$, therefore being a constant of the material. Combining the N_f of all cycles within a flight, the Palmgren-Miner rule was applied to estimate the total damage that each flight would cause to the structure. With the damage dealt and the number of flights for each flight type, the total damage of the block was calculated.

Fatigue life estimation using S-N curve with simple plasticity correction

For the second method, the estimation of fatigue life was similar to the first one with addition of a plasticity correction in cycles that overcome the yield strength of the material. The idea behind this is to adjust only the cycles in which the maximum local stress is higher than yield strength by correcting the σ_{max} and the σ_a as shown in Fig. 5. This adjustment is not considered for subsequent cycles.

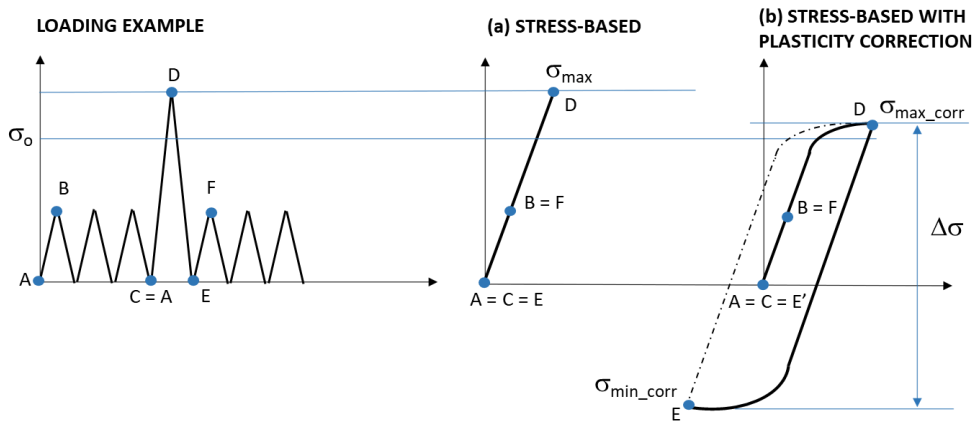

Figure 5 - Simple plasticity correction.

To do that, σ_{max} was determined and if it was higher than the yield strength, the Ramberg-Osgood relation for the cyclic stress-strain curve, coupled with Neuber's rule were solved simultaneously to determine the maximum local stress σ_{max} and the σ_a. This was done by using the material properties and the equations discussed in this section, the σ_{max} and σ_a were determined by reducing the residue (R) of Neuber's rule and Ramberg-Osgood equations attached, as presented in equations below.

$$R = 1000 * \left[\frac{(k_t S_{max})^2}{\sigma_{max} E} - \frac{\sigma_{max}}{E} + \varepsilon_p \left(\frac{\sigma_{max}}{\sigma_y} \right)^{1/n'} \right] \tag{5}$$

$$R = 1000 * \left[\frac{(k_t S_a)^2}{\sigma_a E} - \frac{\sigma_a}{E} + \varepsilon_p \left(\frac{\sigma_a}{\sigma_y} \right)^{1/n'} \right] \tag{6}$$

The equations were multiplied by a factor of 1000 as a way of having a smaller final residue. After getting the adjusted σ_{max} and σ_a, they are converted to nominal stresses and SWT's equation for mean stress correction is used. As the previous method, with S_{ar} and the material properties, N_f is calculated for every cycle and the damage of each flight type is computed.

Fatigue life estimation using ε-N curve

The third approach applied in this work is a strain-based method, so the plasticity effect can be calculated with more accuracy. As early discussed, stress-based approaches generally do not consider plastic deformation, therefore, to have a good prediction of fatigue failure of a structure that surpass yield strength during service life, the mechanical behavior of the material post overload needs to be evaluated, not only for the cycle that it occurs, but also for subsequent cycles due to the permanent effect of a plastic deformation. The steps taken for this method follow the procedure described by Dowling (Dowling, 2012). For every reversal the stresses and strains are calculated by adding Δσ and Δε from the previous point respecting material memory effect.

For the first load, by having the nominal stress S and the geometrical and material properties, a numerical solution of Neuber's rule attached to Ramberg-Osgood is used so σ is obtained. Because the local stress amplitude is determined with equations that already consider mechanical behavior for stresses over yield strength, there is no need to correct the obtained value. After finding the value of σ, the strain ε of this point is calculated through Ramberg-Osgood relation.

$$\varepsilon = \frac{\sigma}{E} + \psi \left(\frac{\psi \sigma}{H'} \right)^{1/n'} \tag{7}$$

where ψ is a unity (1 or -1) that indicates the loading direction. For the next reversals σ and ε are calculated based on ranges.

$$\sigma_Y = \sigma_X + \psi \Delta \sigma_{XY} \tag{8}$$

$$\varepsilon_Y = \varepsilon_X + \psi \Delta \varepsilon_{XY} \tag{9}$$

To obtain these range values, an equation similar to equation 6 is used in which the modification made is to consider amplitudes instead of a single value. Therefore, knowing that $\sigma_a = \Delta\sigma/2$, the values were calculated as follows

$$\Delta S_{XY} = |S_Y - S_X| \tag{10}$$

$$\frac{\Delta S_{XY}}{2} = \frac{1}{k_t}\sqrt{\left(\frac{\Delta\sigma_{XY}}{2}\right)^2 + \frac{\Delta\sigma_{XY}E}{2}\left(\frac{\Delta\sigma_{XY}}{2H'}\right)^{1/n'}} \tag{11}$$

$$\frac{\Delta\varepsilon_{XY}}{2} = \frac{\Delta\sigma_{XY}}{2E} + \left(\frac{\Delta\sigma_{XY}}{2H'}\right)^{1/n'} \tag{12}$$

Is important to remember that the origin point must respect the material's memory effects using the correct previous point to ensure that each loop is respected. After computing σ and ε for every point of the load sequence, rainflow is used to identify what reversals pair making up a cycle. Then, in possession of the needed information, cumulative fatigue damage is calculated using SWT's mean stress correction implemented in a strain-life curve:

$$\sigma_{max}\varepsilon_a = \frac{\sigma'_f}{E}\left(2N_f\right)^{2b} + \sigma'_f\varepsilon'_f\left(2N_f\right)^{b+c} \tag{13}$$

After finding the numerical solution of the previous equation for the number of cycles to failure for every cycle, Palmgren-Miner rule is implemented to acquire the total flight damage.

Results

The results that are presented in Tab. 4 and discussed within this chapter for TWIST and MINITWIST standardized load sequences were achieved after the steps presented in previous sections.

Table 4 - Block damage comparison of TWIST and MINITWIST loading spectra.

Block damage				
kt	Method	TWIST	MINITWIST	Difference (%)
1.0	Stress-based w/o correction	3.43E-06	3.43E-06	8.13E-04
	Stress-based w/ correction	3.43E-06	3.43E-06	8.13E-04
	Strain-based	3.43E-06	3.42E-06	8.13E-04
2.0	Stress-based w/o correction	1.58E-03	1.58E-03	8.13E-04
	Stress-based w/ correction	1.58E-03	1.58E-03	8.13E-04
	Strain-based	1.54E-03	1.54E-03	8.35E-04
2.5	Stress-based w/o correction	1.14E-02	1.14E-02	8.13E-04
	Stress-based w/ correction	1.12E-02	1.12E-02	8.30E-04
	Strain-based	1.05E-02	1.05E-02	8.79E-04
3.0	Stress-based w/o correction	5.72E-02	5.72E-02	8.13E-04
	Stress-based w/ correction	5.23E-02	5.22E-02	8.90E-04
	Strain-based	4.81E-02	4.81E-02	9.67E-04
3.33	Stress-based w/o correction	1.44E-01	1.44E-01	8.13E-04
	Stress-based w/ correction	1.15E-01	1.15E-01	1.02E-03
	Strain-based	1.11E-01	1.10E-01	1.06E-03

Strain-based approach presented the lowest damage per block in all cases analyzed. This is not only due to the correction of plasticity in cycles which overloads occur, but mainly because of the perception of the historic incremental effect in fatigue life caused by overload cycles on posterior ones, a consideration that stress-based methods developed in this work didn't have. It shows that 2024-T351 airplane structures using stress-based methods to estimate their fatigue life and experience some degree of plastic deformation may have a longer life then stipulated. Since reduction of weight is important for the aeronautical industry, 2024-T351 structures in which fatigue life failure is driving the design of the component may be overestimated and present opportunities of improvement.

For the stress-based approach without plasticity correction, the $k_t = 3.0$ has shown the closest block damage in relation what is expected in real life (D≤0,1). Taken this case as a reference, the block damage difference reached a maximum value of 16% when comparing the stress-based approach without plasticity correction with strain-based approach in this case.

Block damage differences in comparison with TWIST method were between 10^{-3} and 10^{-4} in general. The variation remained approximately the same, but as k_t increases all proposed methods who accounted for plasticity effects started to show an increasing of deviation in relation to TWIST results. It worth notice that, when executing the strain-based approach, the time for MINITWIST was nearly 4 times faster than using TWIST spectra.

With these results it's possible to find different moments of application for the three methods discussed in this work. Starting from the stress-based without plasticity correction, this method estimated the lower fatigue life within the three and does not consider some important memory effects. Even though, it estimated values of similar order of magnitude when compared to the other two, and it is the most simple one to be implemented. Therefore, it is a method that may be used when is assured that little or no plasticity occurs during service life, or when fast and not so accurate fatigue estimations are needed.

The stress-based approach with plasticity correction, has presented a value of fatigue damage in between of the two methods. Since it only corrects single cycles and does not have sequential considerations of the load history, it is a more complete method than the traditional stress-based approach in terms of considering the influence of plastic effects on fatigue life, and it is simpler than the strain-based approach. Not only this method is of easy implementation, but for the spectra analyzed in this work it also presented similar block results when compared to the strain-based approach. Thus, it may be suitable for cases when some degree of plasticity is expected, however it's desirable to have a simpler fatigue life estimation.

If it's necessary a fatigue life estimation that considers plasticity and its impact on following load cycles, then the strain-based approach fits better for this occasion. The detrimental of this choice is that due to its complexity its implementation is harder, and the executing time is longer given that to implement the memory effect for every reversal the program must read past data to calculate the next values of σ and ε.

CONCLUSION

The main purpose of this work is to evaluate plasticity effects on fatigue life of aeronautical structures considering a variable amplitude loading scenario. The evaluation of plasticity effects is done by comparing a strain-based approach to two stress-based approaches. Fatigue life estimations are made by the use of Palmgren-Miner cumulative damage rule, and to ensure the loads simulate the spectrum experienced by an airplane, TWIST and MINITWIST standardized load sequences are used.

Analyzing the results discussed in previous chapter, it is possible to draw the following remarks:

- For the applied base load and loading spectra the calculated damages are in accordance with real life scenarios reaching a total damage below 0.1 per block.
- MINITWIST can be used as a faster test option of TWIST, given that for these cases of loading, studied material and k_t values analyzed the lower amplitudes cycles have a small impact in flight damage.
- When plasticity effects are considered, the damage of the most severe flight types, which possess overloads, is reduced, because the resultant stress after the plastic deformation on that cycle is smaller than the one calculated using a perfectly elastic material model.
- For the generated loading, geometries and material analyzed, the less severe flights account for the most part of a block fatigue damage, due to their higher occurrence.
- The strain-based method estimated a lower block damage when compared to the other approaches, therefore a longer fatigue life for the cases analyzed.
- For $k_t = 3$, the closer values of block damage in relation to expected in real life, the strain-based method had 16.0% difference when compared to the stress-based method without plasticity correction. Thus, when fatigue is limiting the design of an aeronautical structure, the impact of plasticity must be considered.

ACKNOWLEDGMENTS

The first author would like to thank Embraer and ITA for developing the Engineering Specialization Program (PEE), which represents an example of training professionals for the market; to his advisors: Mariano Andrés Arbelo and Carlos Eduardo Chaves, for having actively participated throughout the development of the work, even with the absence of face-to-face meetings; to MSc. Juliana Diniz for taking the time to clarify doubts on some occasions and Fundação Casimiro Montenegro Filho for making it possible for me to remain in the program.

The authors would like to thank the entire PEE coordination team (especially Nolf, Fabiana and Jenifer), who always sought to help participants by giving all the necessary support and promoting a healthy environment so that we could carry out our activities.

This work was supported by CNPq Grant No. 311972/2020-9.

REFERENCES

ASTM. E1049 − 85 Standard practices for cycle counting in fatigue analysis. [S.l.]. 2011.

BELKHIRIA, S.; HAMDI, A.; FATHALLAH, R. Strain-based criterion for uniaxial fatigue life prediction for an SBR rubber: comparative study and development. Proceedings of the Institution of Mechanical Engineers, Part L: Journal of Materials: Design and Applications, v. 234, n. 7, p. 897-909, 2020.

BÖHM, E. et al. Accumulation of fatigue damage using memory of the material. Procedia Materials Science, v. 3, p. 2-7, 2014.

BRANCO, R. et al. Comparison of different one-parameter damage laws and local stress-strain approaches in multiaxial fatigue life assessment of notched components. International Journal of Fatigue, v. 151, p. 106405, 2021.

BUCH, A. Effect of some aircraft loading program modifications on the fatigue life of open hole specimens. Engineering Fracture Mechanics, v. 13, n. 2, p. 237-256, 1980.

CHEN, J.; YAO, W.; GAO, D. Fatigue life evaluation of tension-compression asymmetric material using local stress–strain method. Fatigue & Fracture of Engineering Materials & Structures, v. 43, n. 9, p. 1994-2005, 2020.

DOWLING, N. E. Mean stress effects in strain–life fatigue. Fatigue & Fracture of Engineering Materials & Structures, v. 32, n. 12, p. 1004-1019, 2009.

DOWLING, N. E. Mechanical behavior of materials: engineering methods for deformation, fracture, and fatigue. Harlow, England: Pearson E ducation Limited, 2012.

DE JONG, J. B. et al. A standardized load sequence for flight simulation tests on transport aircraft wing structures. NLR-TR 73029 U, LBF Bericht FB-106, 1973.

ESDU. Standard fatigue loading sequences. [S.l.]. 2003.

FATEMI, A.; YANG, L. Cumulative fatigue damage and life prediction theories: a survey of the state of the art for homogeneous materials. International journal of fatigue, v. 20, n. 1, p. 9-34, 1998.

GARCÍA-RUBIO, M. et al. Influence of molybdate species on the tartaric acid/sulphuric acid anodic films grown on AA2024 T3 aerospace alloy. Corrosion Science, v. 51, n. 9, p. 2034-2042, 2009.

HEULER, P.; KLÄTSCHKE, H. Generation and use of standardised load spectra and load–time histories. International Journal of Fatigue, v. 27, n. 8, p. 974-990, 2005.

KWOFIE, S.; RAHBAR, N. A fatigue driving stress approach to damage and life prediction under variable amplitude loading. International Journal of Damage Mechanics, v. 22, n. 3, p. 393-404, 2013.

LI, S.; CUI, W.; PAIK, J. K. An improved procedure for generating standardised load-time histories for marine structures. Proceedings of the Institution of Mechanical Engineers, Part M: Journal of Engineering for the Maritime Environment, v. 230, n. 2, p. 281-296, 2016.

LIAO, D. et al. Recent advances on notch effects in metal fatigue: A review. Fatigue & Fracture of Engineering Materials & Structures, v. 43, n. 4, p. 637-659, 2020.

LIU, J. et al. The effect of holes quality on fatigue life of open hole. Materials Science and Engineering: A, v. 467, n. 1-2, p. 8-14, 2007.

LOWAK, H. et al. MINITWIST: A shortened version of TWIST (Transport WIng STandard Load computer programme). NLR MP 79018 U, 1979.

MADURO, L. P. et al. Modeling the growth of LT and TL-oriented fatigue cracks in longitudinally and transversely pre-strained Al 2524-T3 alloy. Procedia Engineering, v. 10, p. 1214-1219, 2011.

NEUBER, H. Theory of stress concentration for shear-strained prismatical bodies with: arbitrary nonlinear stress-strain law. [S.l], 1961.

PENG, Z. et al. A new cumulative fatigue damage rule based on dynamic residual SN curve and material memory concept. Metals, v. 8, n. 6, p. 456, 2018.

QIAO, H.; HAO, X. Two-parameter nominal stress approach. International journal of fatigue, v. 17, n. 5, p. 339-341, 1995.

REGE, K.; PAVLOU, D. G. A one-parameter nonlinear fatigue damage accumulation model. International Journal of Fatigue, v. 98, p. 234-246, 2017.

SCHIJVE, J. Fatigue of structures and materials. [S.l], 2009.

SCHIJVE, J. Fatigue of aircraft materials and structures. International Journal of Fatigue, v. 16, n. 1, p. 21-32, 1994.

SKINN, D.; MIEDLAR, P.; KELLY, L. Flight Loads Data for a Boeing 737-400 in Commercial Operation. Dayton OH: Univ. Research Inst, 1996.

ZHAO, Y. X.; YANG, B.; ZHAI, Z. Y. The framework for a strain-based fatigue reliability analysis. International Journal of Fatigue, v. 30, n. 3, p. 493-501, 2008.

ZHOU, J. et al. A novel non-linear cumulative fatigue damage model based on the degradation of material memory. International Journal of Damage Mechanics, v. 29, n. 4, p. 610-625, 2020.

RESPONSIBILITY NOTICE

The author(s) is (are) the only party(ies) responsible for the printed material included in this paper.